Taylor & Francis
Taylor & Francis Group

RESEARCH ARTICLE

Chitosan-dipotassium orthophosphate lyophilizate: a novel *in situ* thermogel carrier system of allogeneic platelet lysate growth factors

Toaa A. Abdelrahman, Amira Motawea, Marwa S. El-Dahhan and Galal M. Abdelghani

Department of Pharmaceutics, Faculty of Pharmacy, Mansoura University, Mansoura, Egypt

ABSTRACT

The clinical success of platelet-rich plasma (PRP) is constrained by its limited mechanical strength, rapid disintegration by lytic enzymes, and the consequent short-term release of bioactive growth factors (GFs). Recently, attempts to formulate PRP and other hemoderivatives, such as platelet lysate (PL) have been underway. The current study aimed to formulate allogeneic freeze-dried human platelet lysate (HPL) onto lyophilized chitosan - dipotassium hydrogen orthophosphate (CS/DHO) thermo-sensitive scaffolds. A systemic approach was employed to optimize freeze-drying (FD) procedures targeting predefined critical quality attributes (CQAs). Thermal behavior, vibrational spectroscopy, morphological and moisture content analyses were used to detect possible protein destabilization during formulation and suboptimal cake properties. The effect of CS/DHO concentrations on thermo-responsiveness and release kinetics were investigated. Finally, six-months stability and cytotoxicity studies were carried out. An optimized lyophilizate was attainable with residual moisture of less than 5% and thermoresponsive to 33 °C in less than 3 min. HPL proteins were sustainedly released over five days in a pH-sensitive manner. The stability study indicated plausible physical and biochemical stability. Cell viability testing supported the cytocompatibility of the system. Finally, the lyophilizate variant of CS/DHO thermogel overcomes limited storage stability previously posed as a challenge in freshly prepared thermogels. The developed system overcomes the drawbacks of currently used PRP treatment and provides a novel GF-rich scaffold for wound repair.

GRAPHICAL ABSTRACT
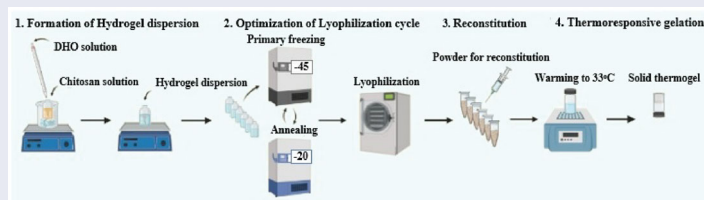
1. Introduction

For several decades, the use of hemoderivatives in the management of acute and chronic wounds has gained increasing attention of researchers and clinicians (Carter & Fylling, 2011; Sumner et al., 2017). Since the late 1990s, autologous platelet-rich plasma (PRP) has been used in several wound healing applications including musculoskeletal injuries, and corneal ulceration (Anitua et al., 2013; Belk et al., 2021). PRP contains supraphysiological concentrations of growth factors (GFs), chemokines and cytokines which impart a powerful wound healing activity such as platelet-derived growth factor (PDGF), vascular endothelial growth factor (VEGF), epidermal growth factor (EGF), fibroblast growth factor (FGF), transforming growth factor (TGF) and insulin-like growth factor (IGF) (Sundman et al., 2011). GFs and cytokines act by means of chemotactic interactions on a cellular level to induce cell migration, epithelialization, angiogenesis, granulation, and wound contraction (Fernandez-Moure et al., 2017). A few recombinant GF formulations are available on the global market for use in wound-healing applications such as Regranex®, Easyef®, Fiblast®, and Chemicon®. Apart from their excessive cost, some of these products have been labeled for their potential to induce cancerous cell growth. In light of the above, PRP is an attractive choice given its relative safety to other treatments especially recombinant growth factor formulations (Amable et al., 2013). Moreover, minimal cost is inferred for PRP production as it is easily obtained from fresh blood.

Albeit the above-mentioned advantages, the clinical application of PRP is challenged by the premature bolus release of bioactive GFs which have short circulation times. Studies

have shown that this bolus delivery can reach a peak of ~70% of the PRP bioactive molecules within 10 min of contact with the wound micro-environment (Anitua et al., 2012). Moreover, PRP has a short half-life due to the presence of proinflammatory cells that release special enzymes known as matrix metalloproteinases (MMPs). In turn, MMPs create a proteolytic microenvironment that actively breaks down GFs and cytokines in their proximity causing flush-out from the application site within 1 to 2 h (Marx, 2001). Commonly, PRP is applied to a wound in the form of a liquid, which makes its tissue residence time limited. Given these limitations, frequent dosing and higher doses may be required in order to render PRP treatment effective. This is impractical due to the need of multiple blood harvesting procedures, increasing bed-side time and patient discomfort (Oneto et al., 2021). In light of this, allogeneic hemoderivatives may offer a reasonable alternative especially given their comparable efficacy (He et al., 2020).

Thermosensitive in situ gels are attractive polymeric systems as they allow physical entrapment of target molecules using mild formulation conditions. This is a simplistic approach compared to other complex formulation techniques that may entail the use of organic solvents or drastic formulation conditions especially when working with hydrophilic macromolecules such as proteins and GFs. Thermoresponsive gels exist in a liquid form at ambient temperature, and when exposed to body temperature, sol-to-gel transition occurs forming gel implants that gradually elute bioactive cargo to the application site (Jain et al., 2017).

Chitosan (CS) is a natural aminated polysaccharide that is classified as generally recognized as safe (GRAS) by the Food and Drug Administration (FDA). Recently, much attention has been paid toward the application of CS-based thermoresponsive smart gels as ideal platforms in tissue engineering applications. This is ascribed to good biocompatibility, low immunogenicity, ability to absorb exudates and film forming properties (Liu et al., 2016).

In 2000, Chenite et al fabricated a thermoresponsive CS hydrogel by mixing acidic CS solution with an organic polyol salt; β-glycerophosphate (β-GP) (Chenite et al., 2000). The authors attributed the thermo-responsive nature of the system to heat-induced proton transfer from cationic polymeric chains to the polyol moiety. Ta et al. (2009) further ameliorated the above concept by formulating a CS/dipotassium hydrogen orthophosphate (CS/DHO) thermogel system (Ta et al., 2009). This precluded the need for a polyol moiety to impart thermo-responsiveness. The uniqueness of such systems resides in the ability to form a near-neutral liquid gel dispersion of CS at room temperature without causing its precipitation. Heat-induced deprotonation of CS chains results in a homogeneous sol-to-gel transition of the system via promoting CS/CS hydrophobic interactions and hydrogen bonding. This contrasts to ionic crosslinking with polyanions such as sodium tripolyphosphate (Casettari et al., 2013). Temperature-controlled gelation of other CS-inorganic di-anionic phosphate-based dispersions was attainable by Casettari et al. (2013), Nair et al. (2007).

A main setback of such systems is limited physical stability. Moreover, little attention was offered to the preservation of the bioactivity of the cargo upon long-term storage. Ruel-Gariépy et al. (2000) reported spontaneous gelation of CS/β-GP system after 2 to 3 months for refrigerated samples. At room temperature, samples prepared with CS with a higher degree of deacetylation started to show spontaneous gelation as early as 3 days of storage (Ruel-Gariépy et al., 2000). In this study, the conformational stability of the model proteins used was not reported on.

In 2016, Wu et al developed a lyophilized variant of the CS/β-GP thermogel system as an attempt to enhance the physical stability of the system (Wu et al., 2016). After 3 months of storage, CS/β-GP lyophilizates were reconstituted to liquid hydrogel dispersions that retained the native pH and gelation time of the freshly prepared samples. This was true for refrigerated and ambient storage conditions. Again, a study of the conformational stability of model proteins was not conveyed.

Freeze-drying (FD) is frequently used as a strategy to enhance the long-term storage stability of sensitive biopharmaceuticals (Santana et al., 2014). A typical FD cycle would constitute four stages: freezing, annealing, primary drying and secondary drying (Rathore and Rajan, 2008). The development of a robust freeze-drying cycle (FD cycle) entails the determination of critical parameters that impact product critical quality attributes (CQAs) (U.S. Department of Health and Human Services Food and Drug Administration, 2009). A non-optimized FD-cycle can compromise product appearance and shelf-life stability as well as sustain excessive production costs. Hence it is primitive to carefully design a FD cycle that is able to fulfill two main pre-requisites: 1) biopharmaceutical stabilization, 2) pharmaceutically elegant product.

2. Materials

Low M.W. chitosan (CS) (50–190 kDa) was purchased from Sigma Aldrich, St. Louis, MO, USA. Dipotassium hydrogen orthophosphate salt (DHO), mannitol (Man) and sucrose (Suc) were supplied from El-Nasr Chemicals, Cairo, Egypt. Glacial acetic acid was acquired from Merck, Darmstadt, Germany. Human PDGF-BB Enzyme-linked Immunosorbent Assay (ELISA) Kits, Invitrogen, BMS2071 was obtained from Thermo Fisher Scientific, USA. Leukocyte-reduced human platelet concentrates (PCs) were kindly donated by Mansoura University Blood Bank. Upon good intentions, the PCs were kept in a shaking incubator at ambient temperature until past the expiry date before use in experiments. Human Skin Fibroblast American Type Culture Collection (HSF ATCC) cell line was obtained from Nawah Scientific Inc., Mokatam, Cairo, Egypt. Cells were maintained in Dulbecco's Modified Eagle Medium (DMEM) media supplemented with 100 mg/mL of streptomycin, 100 units/mL of penicillin and 10% of heat-inactivated fetal bovine serum in humidified 5% (v/v) CO_2 atmosphere at 37 °C until use. All other chemicals and reagents were of fine analytical grade and used without further purification. All research reported herein is approved by

and complies with the guidelines of the Research Ethics Committee, Faculty of Pharmacy, Mansoura University.

3. Methodology

The study aimed to fabricate human platelet lysate (HPL) in a controlled-release thermoresponsive gel that is highly biocompatible, potently bioactive, and has a feasible shelf-life for use in wound healing applications. HPL was prepared based on a method previously reported by Schallmoser et al (Schallmoser & Strunk, 2009). PDGF-BB was chosen as a representative of the GF composition of HPL given its cardinal role in wound healing (Fekete et al., 2012). PDGF-BB recovery percentage was calculated in order to reveal any loss of bioactivity caused by FD of PC. HPL was then loaded onto a CS/DHO hydrogel dispersion, and the preparation was freeze-dried to form a lyophilizate. To the best of our knowledge, this is the first attempt to formulate a CS/DHO thermosensitive lyophilizate. To this effect, an optimized FD procedure to maximize system physical and biological stability was developed and parameters affecting CQAs of the formulation were investigated based on a QbD approach (U.S. Department of Health and Human Services Food and Drug Administration, 2009). This was complemented with differential scanning calorimetry (DSC) as one of the most common thermal analysis methods used to refine the FD cycle of protein-based formulations. Also, X-ray powder diffraction (XRPD) and Fourier transform infrared (FT-IR) analyses of the lyophilizates were employed to characterize certain stability predictors such as bulking agent polymorph species and protein secondary structure, respectively (Remmele et al., 2012). The release behavior of the system was comprehensively investigated by analysis of total protein (TP) as well as PDGF-BB release patterns. Finally, cell viability testing was performed on human skin fibroblast (HSF) cells to confirm the safety of the formulation under development. Our goal is to provide a starting point for the development of stable lyophilized HPL formulations as a new and promising outlook to wound healing.

3.1. Preparation of lyophilized human platelet lysate (HPL)

PC was activated by means of three freeze-thaw cycles to induce platelet breakdown, α-particle degranulation, and release of GFs. For each freeze-thaw cycle, the PC was frozen at $-80\,°C$ overnight and then allowed to thaw at $37\,°C$ for 4 hrs (Strandberg et al., 2017). The PC was then portioned into sterile 50 mL falcon tubes and centrifuged at $4\,°C$ at 5000 rpm for 15 minutes. The supernatant, now on referred to as human platelet lysate (HPL), was decanted into sterile petri dishes that were then frozen at $-20\,°C$ overnight. HPL was then freeze-dried under vacuum for 12 hrs at $-54\,°C$ shelf temperature (Freeze dryer, SIM FD 8-8 T, SIM international, USA) to obtain lyophilized HPL which was then stored at $-20\,°C$ for further experimental use (Schallmoser and Strunk, 2009).

PDGF-BB was quantified in aliquots of fresh PC and HPL to determine baseline levels of the GF. In addition, the lyophilizate of 3 mL of HPL was reconstituted using normal saline to original volume and tested for PDGF-BB using the following equation [20]:

$$R(\%) = \frac{PDGF-BB\ ELISA\ of\ lyophilized\ HPL}{PDGF-BB\ ELISA\ of\ HPL} \times 100$$

where, R(%) is the percentage recovery of PDGF-BB as quantified using ELISA.

3.2. Preparation of CS and DHO solutions

CS stock solution (3% w/v) was prepared by incrementally adding CS powder to 0.3 M acetic acid under continuous magnetic stirring (Hot Plate and Magnetic stirrer, Misung Scientific Co., LTD, Korea). The mixture was stirred overnight at room temperature to ensure complete dissolution. The pH of the solution was adjusted to 5.5 ± 0.2 using 0.1 M sodium hydroxide solution. This stock solution was then diluted with water to 2% and 1.5% CS for subsequent experiments. Likewise, a DHO stock solution (50% w/v) was prepared, and pH was adjusted to 9.5 ± 0.2 using 0.1 M sodium hydroxide solution. The stock solution was then diluted to working concentrations of DHO at 15%, 20% and 25%. All solutions were filtered through 0.45 µm Millipore filter and stored under refrigeration for further experimental use.

3.3. Preparation of CS/DHO hydrogel dispersions

Five milliliters of chilled CS solution was placed in a vial immersed in an ice bath. 0.5 ml of ice-cold DHO solution of different concentrations was added dropwise to the CS solution under magnetic stirring to form CS/DHO gel dispersion. For the preparation of medicated CS/DHO gel solutions, lyophilized HPL was first dispersed into the CS solution at a concentration of 1%w/v and magnetically stirred until complete dissolution. The salt solution was then added as mentioned above. Using the above procedure, final CS concentrations of either 1.4% or 1.8% and DHO concentrations of 1.5%, 2.0% or 2.5% were achieved as indicated in Table 1 for formulae F1 to F6. Gel dispersions where then prepared for FD as elaborated below.

3.4. Preparation of CS/DHO lyophilizate

In preparation for FD, frozen samples were removed from $-45\,°C$ freezer and placed on pre-cooled FD shelves at a temperature of $-54\,°C$ and vacuum immediately applied to avoid any rise in product temperature (Tp). As indicated in Table 1, F3 constituted the highest solid content which made it most susceptible to FD defects such as cake collapse

Table 1. Formulations tested at different CS and DHO concentrations.

Formula	CS Conc. (%w/v)	DHO Conc. (%w/v)
F1	1.8	1.5
F2	1.8	2.0
F3	1.8	2.5
F4	1.4	1.5
F5	1.4	2.0
F6	1.4	2.5

Table 2. Freeze-drying protocols investigated for F3 at a fixed Man: Suc of 6:2%w/v.

FD protocols	Freezing		Annealing		Primary Drying		Secondary Drying	
	Temperature (°C)	Duration (hrs)	Temperature (°C)	Duration (hrs)	Temperature (°C)	Duration (hrs)	Temperature (°C)	Duration (hrs)
Unannealed	−20	24	–	–	−54	12	–	–
Conservative	−45	18	−20	6	−54	12	–	–
Extensive	−45	18	−20	6	−54	12	ambient	2 hrs

and incomplete dissolution (Cao et al., 2013). Hence, F3 was used to test for optimum cryoprotectant levels and FD conditions as well as for subsequent lyophilizate characterization. Samples were prepared in triplicates for each testing procedure.

3.5. Optimization of the FD cycle

3.5.1. Cryoprotectants
Man and Suc were used as bulking and stabilizing agents, respectively. Three Man: Suc concentration ratios were tested: 4:1, 4:2, and 6:2%w/v (Cao et al., 2013). To determine the optimum cryoprotectants levels, samples were prepared with each of the above ratios, frozen at −20 °C overnight then freeze-dried for 12 hrs (unannealed FD procedure), as detailed in Table 2.

3.5.2. FD conditions
Three different FD protocols were investigated by varying freezing, annealing, primary and secondary drying conditions as elucidated in Table 2. First, an unannealed FD procedure was applied to F3. In addition, a conservative FD procedure with a low-temperature annealing step as well as an extensive FD procedure with low- and high- annealing steps were also investigated for the same formulation. For a direct comparison of the efficiency of the FD conditions, fixed Man: Suc amounts of 6:2%w/v, respectively were added.

Optimum excipient concentration ratio and FD conditions were decided based on predefined CQAs, namely, cake appearance, residual moisture content and reconstitution time as detailed below (Haeuser et al., 2020).

3.6. CQA testing of the lyophilizate

3.6.1. Macroscopic appearance
Lyophilizates were carefully checked for any aggregation, ridge formation or cake collapse. Samples showing such defects were excluded from further testing. Representative pictures were taken using a camera.

3.6.2. Residual moisture
Residual moisture content was analyzed using a Moisture Analyzer (Mettler Toledo HS153, Greifensee, Switzerland). The samples were placed in the sample pan holder and heated at 100 °C to ensure complete drying. The weight of each sample was monitored dynamically on the digital screen until no further decrease in weight was observed. The moisture content (%) displayed on the digital screen was then noted. Triplicate samples were tested, and residual moisture content was reported as mean ± SD.

3.6.3. Reconstitution time
Each lyophilizate was reconstituted to original volume using normal saline by inserting a 5 mL disposable syringe equipped with 26-G needle into the vial. The dispersion was agitated by repeatedly injecting and withdrawing into the stoppered vial and was then left to hydrate. Complete dissolution was assessed visually. Reconstitution time was only measured for samples that were completely dissolved based on triplicate samples expressed as mean ± SD.

3.7. Characterization of the lyophilizate

3.7.1. Differential scanning calorimetry (DSC)
The DSC scan of F3 lyophilizate was conducted using differential scanning calorimetry (Pyris[TM] 6 DSC, Perkin Elmer, USA) calibrated with indium. Approximately 2 mg of crushed cake were crimped into aluminum crucibles and sealed hermetically. Samples were scanned from 25 °C to 150 °C at a ramp rate of 10 °C/min, as previously reported by Assegehegn et al with a slight modification (Assegehegn et al., 2020). The DSC thermogram of the lyophilizate were inspected for occurrence of crystallization exotherms and endothermic transitions indicative of glass transition temperature (Tg) of the lyophilizate. The Tg was determined as the midpoint of the endothermic transition using Origin, 2021, OriginLab Corporation, Northampton, MA, USA (Assegehegn et al., 2020).

3.7.2. X-Ray powder diffraction (XRPD)
The phase behavior of F3 lyophilized cakes was investigated using XRPD. An X-ray diffractometer (Rigaku Denki, Rint-2500VL. Tokyo, Japan) equipped with Cu-Kα (λ = 1.5424 Å) radiation scanned from 3° to 55° at 2θ angle with a step of 0.02° was used for this analysis. The diffractogram of the F3 lyophilizate was examined for detection of Man polymorphs. The diffractogram of lyophilized 6% Man solution was used as a reference taking into consideration that it mainly constitutes β-Man polymorph which is the only stable form of Man (Horn et al., 2018). The existence of β-Man polymorph in the formulation was detected using its main reference peaks: (10.4°, 14.6°, 16.8°, 18.8°, 20.3°, 23.4°) (Horn et al., 2018). Peaks used for identification are underlined.

3.7.3. Fourier-transform infrared spectroscopy (FT-IR)

FT-IR spectra were collected for the freeze-dried cake of F3 on a FT-IR spectrophotometer (Thermo Fisher Scientific, Inc., Waltham, MA, USA). FT-IR spectra for samples of pure CS and HPL powders were used as references of native peaks. The samples were grounded into fine powder before mixing with KBr powder and compacted into pellets for FT-IR examination. The scanning wave range was 400 to 4000 cm^{-1} (Lewis et al., 2010).

3.8. Gelation time and thermal reversibility test

The gelation times of CS/DHO lyophilizates for formulae F1 to F6 were measured at a constant temperature using the test tube inversion method (Bhattarai et al., 2005). CS/DHO solutions (3 mL per vial) were placed in a water bath maintained at a temperature of $33 \pm 1\,^\circ C$ and samples flowability was monitored every 30 s by tilting the vials. The sol-gel transition point was taken as the time of non-flow of the sample upon inversion of the vial. To check the thermoreversibility of the hydrogels, samples were then allowed to equilibrate at room temperature for 15 min and flowability was checked. If the gels returned to a liquid state, they were considered thermo-reversible hydrogels.

3.9. In-vitro *release study*

HPL-loaded CS/DHO lyophilizates were reconstituted to a volume of 3 mL using normal saline and were incubated at $33\,^\circ C \pm 1\,^\circ C$ for 30 min to ensure complete gelation. 5 mL phosphate buffered saline (PBS) was carefully placed on top of the thermogels then samples were gently shaken at 100 rpm in a shaking incubator (GFL Gesellschaft für Labortechnik, Burgwedel, Germany) (Bernal-Chávez et al., 2020). At predetermined intervals, the entire PBS solution was carefully pipetted out of the sample vials without interrupting the gel surface and used for TP and PDGF-BB analyses as detailed below. The release medium was replenished with a fresh aliquot to maintain sink conditions and the release experiment was continued (Wu et al., 2016).

To study the effect of pH on the release behavior of the system, a release study was conducted at two different pH levels to represent a non-infected and an infected wound: pH 6.5 and pH 7.4, respectively (Bullock et al., 2020).

Another release experiment was conducted to study the effect of varying CS and DHO concentrations on the release rate. Final DHO concentrations of 1.5%, 2% and 2.5% and final CS concentrations of 1.5% and 2% were used to prepare the thermogels for this experiment (F1 to F6). All release data were fitted to zero and first order release models, in addition to Higuchi, Korsmeyer Peppas, Weibull, and Hixson Crowell kinetic models to understand the release behavior of the system (Hixson & Crowell, 1931; Higuchi, 1963; Langenbucher, 1972; Korsmeyer et al., 1983).

3.9.1. TP and PDGF-BB quantitation

TP release was quantified by means of a pre-developed calibration curve for UV-absorbance at λ_{max} of 280 nm (UV-VIS Spectro double beam, Labomed Inc., USA) (Bernal-Chávez et al., 2020). The amount of HPL released at each time point was calculated using a pre-set calibration curve. Cumulative release (%) at a specific time point was calculated by accumulating the total HPL release up to that time.

PDGF-BB released was quantified using Human PDGF-BB ELISA kits as per manufacturer instructions with a slight modification. Briefly, a standard calibration curve was established using 7 serial dilutions of PDGF-BB standard. PDGF-BB concentration was determined based on the absorbance of the colored product resultant of the interaction between tetramethyl benzidine (TMB) substrate and sandwiched PDGF-BB at 450 nm. The cumulative release (%) of PDGF-BB at a specific time was calculated as mentioned above for TP. Based on the outcomes of the aforementioned experiments, F3 was selected for further evaluation.

3.10. Cytotoxicity assay

Cytotoxicity was assessed by WST-1 assay using Abcam®kit (ab155902WST-1 Cell Proliferation Reagent). The extent of toxicity was evaluated by measuring the viability of cells cultured in the media containing HPL-loaded CS/DHO dispersions. Briefly, aliquots of 50 μL cell suspension (3×10^3 cells) were seeded in 96-well plates and incubated in complete media for 24 hrs. Each cell was then treated with another aliquot of 50 μL media containing the freeze-dried formulation at serial concentrations of HPL (0.01, 0.1, 1, 10 and 100 μg/mL). After 48 hrs of exposure, cells were treated with 10 μL WST-1 reagent and the absorbance was measured after 1 hour at 450 nm (A_{450}) using a BMG LABTECH®- FLUOstar Omega microplate reader (Allmendgrün, Ortenberg). Representative phase-contrast images of cells were captured just before the addition of WST-1 reagent (Olympus BX 41 microscope, Olympus, USA). The cytotoxic effect was expressed as % cell viability and was used to construct a dose-response curve. Then, the half maximal inhibitory concentration (IC50) in comparison with the untreated (control) cells was calculated from this curve. Cell viability % was calculated in relation to a control of blank formulation using the following equation:

$$Cell\ Viability\ \% = \frac{A_{450}\ of\ treated\ cells}{A_{450}\ of\ control\ cells} \times 100$$

Where A_{450} is the absorbance of the cells at $\lambda = 450$ nm.

3.11. Stability of CS/DHO lyophilizate

The stability of the thermogel system was studied where glass vials with the optimized lyophilizate were stored under refrigerated conditions ($2-8\,^\circ C$) (Anitua et al., 2015). At preset times (1, 2, 3, 4, 8, 16, 20, and 24 weeks), each sample was visually inspected for any physical changes. At maturation, lyophilizates were reconstituted to the original volume using saline and then stored at $-20\,^\circ C$ until the end of the

stability experiment. After six months, the reconstituted samples were thawed at ambient temperature and tested for PDGF-BB content using the ELISA procedure detailed earlier. All measurements were done in triplicate.

3.12. Statistical analysis

All data for the gelation time, moisture content, release profile and stability studies are expressed as mean ± SD. A ρ-value < .05 was set to indicate statistical significance. One-way ANOVA followed by Tukey's post-hoc test was applied to analyze gelation time, moisture content and reconstitution time results. Repeated measures ANOVA was used for release profile and stability results analyses. All statistical analyses were performed using MS Excel 365. KinetDS software was used to study the release kinetics (Mendyk et al., 2012).

4. Results

4.1. System design and optimization

4.1.1. Quality determination of lyophilized HPL
The PDGF-BB content in HPL was found to be 119.9% ± 4.38% compared to fresh PC aliquot. Moreover, the percentage recovery of PDGF-BB was determined to be 90.8% ± 2.53%, based on ELISA testing of lyophilized HPL compared to HPL before lyophilization.

4.1.2. Preparation of CS/DHO lyophilizate
Based on our preliminary studies, CS concentrations higher than 2% w/v failed to form a liquid hydrogel system at room temperature. Also, concentrations of less than 1.5% w/v were unable to exhibit thermo-gelation within a reasonable time of exposure to 33 °C ± 1 °C (data not shown). Similarly, DHO concentrations of less than 1.5% in the hydrogel dispersion were unable to thermogel within a clinically relevant time. Concentrations higher than 2.5% mg/mL formed highly viscous gels that were semi-solid at room temperature (data not shown). Hence final concentrations of 1.5% and 2% w/v CS and 1.5%, 2% and 2.5% DHO were used to prepare F1 to F6 gel dispersions for subsequent studies to investigate gelation time and release behavior.

Given the above-mentioned CS and DHO combinations, F3 was chosen for FD optimization and lyophilizate characterization. This was to prevail any FD defects that could occur in such a lyophilizate at highest CS and DHO levels.

Based on the FD cycle optimization, samples showed varying product quality depending on the cryoprotectant ratio as well as the FD conditions as shown in Figure 1 and Table 3. Visual inspection of samples prepared using Man: Suc at 4:1 and 4:2%w/v, revealed particulates with large apparent size as illustrated in Figure 1(A). These samples were unable to fully dissolve upon reconstitution possibly due to micro-collapse. This was slightly alleviated for samples prepared with a higher concentration of Man at 6%w/v but still partially existent. In addition, all samples lyophilized using unannealed FD failed to pass the CQA testing. All samples showed prominent collapse as shown in Figure 1(B), and

consequently were unable to fully hydrate and dissolve. Including a low-temperature annealing step at −20 °C in protocol 2 allowed for a more efficient primary drying phase with residual moisture content dropping to ∼4%, compared to ∼10% in non-annealed samples. Addition of a high-temperature annealing step via secondary drying at ambient temperature, resulted in a slight reduction in the moisture content of around 0.5%, which was not significant yet, enhanced the lyophilized cake appearance. Consequently, the samples prepared with annealed FD protocols at maximal Man: Suc concentration of 6:2%w/v were able to completely hydrate and dissolve showing no apparent aggregates and had short reconstitution times of around 3 and 2 min, for conservative and extensive annealed FD, respectively. As displayed in Figure 1(C), cake appearance was greatly enhanced yielding a pharmaceutically elegant product.

Based on the above results, it was concluded that bulking (Man)/stabilizing agent (Suc) strength of 6:2%w/v, respectively in addition to extensive FD should be adopted.

4.2. Characterization of the lyophilizate

#### 4.2.1. Differential scanning calorimetry (DSC)
As elucidated in Figure 1(D), the obtained DSC thermograms of F3 lyophilized cakes manifested a lack of crystallization exotherm for Man. This was anticipated as Man was expected to be mostly crystalline in the freeze-dried product as intended by the low- and high- temperature annealing stages (Horn et al., 2018). The Tg of the lyophilized cake was detected at around 45 °C signified by the low-energy step-down peak.

4.2.2. X-Ray powder diffraction (XRPD)
XRPD was used to study the diffraction planes of the system. On confrontation to pure Man diffractogram (Figure 1E i), the presence of β-Man polymorph was confirmed using 3 reference peaks as shown in Figure 1(E) ii, indicating a crystalline scaffold formed by β-Man in F3 lyophilizate. A minor bifurcated peak indicating the presence of δ-Man polymorph was also detected at 22°.

4.2.3. Fourier transform infrared spectroscopy (FT-IR)
The FT-IR spectral investigation for HPL, CS and F3 lyophilizate is shown in Figure 1(F) i, ii and iii, respectively. The spectra elucidate the position of typical protein solid-state amide I and II absorbance bands at 1544 cm^{-1} and 1654 cm^{-1} respectively, were detected for F3. Since CS is also aminated, it was impossible to decipher the amide II band of F3 depicted at 1654 cm^{-1} into individual amide II bands originating from CS and HPL. It is worthy to note that reduced amide bands intensities are expected for the formulation given only 1% and 2% of HPL and CS, respectively in F3 lyophilizate, whereas CS and HPL spectra are for pure powders. Moreover, a slight shift of the amide I bending vibration band from 1544 cm^{-1} to 1568 cm^{-1} was detected in F3.
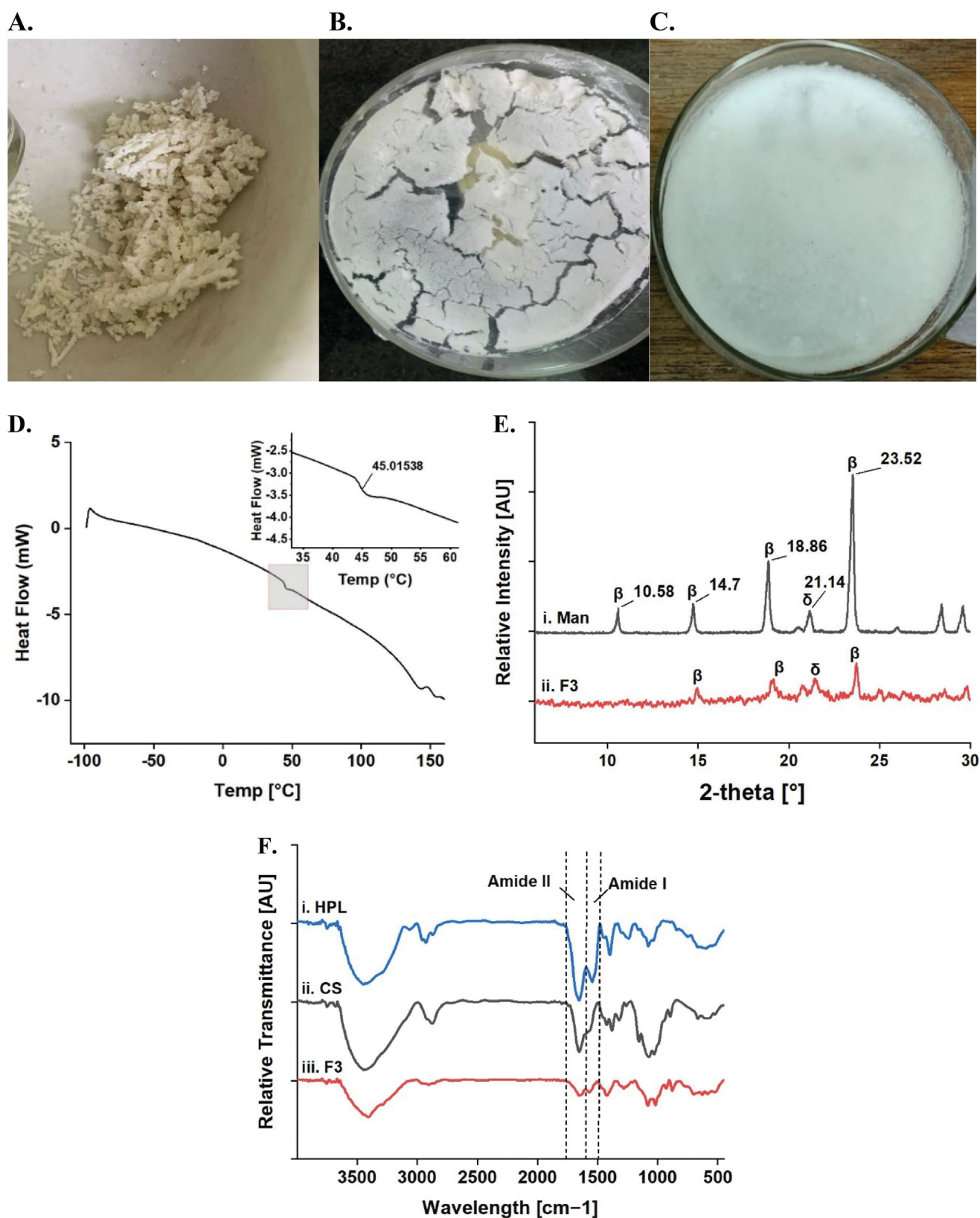
Figure 1. Lyophilizate optimization and characterization. (A) Particulate sample subjected to suboptimal FD cycle, (B) Cake collapse with prominent ridge formation and (C) Optimized FD formulation with crystalline Man scaffold, (D) DSC thermogram of F3, (E) X-ray diffractograms of (i) Man and (ii) F3, and (F) FT-IR spectra for (i) HPL, (ii) CS and (iii) F3.

4.3. Adjustable gelation time

CS/DHO system existed in a liquid state at ambient temperature, showing sol-to-gel transition at $33\,°C \pm 1\,°C$ determined using vial inversion test. Table 4 illustrates the gelation time of F1 to F6 prepared using two CS concentrations (1.4% and 1.8% w/v) and three DHO concentrations (1.5%, 2% and 2.5%). The gelation time of the lyophilizate system was

Table 3. CQA outcomes for optimization of cryoprotectants levels and FD procedure.

Parameter	Critical Quality Attribute (CQA)			
	Cake appearance	Residual moisture (%)	Reconstitution Product	Reconstitution time (min)
Man: Suc (% w/v)	**All samples prepared using unannealed FD protocol**			
4:1	Granular with large aggregates	11.34 ± 3.63	Significant precipitation	N/A
4:2	Granular with large aggregates	9.81 ± 2.85	Significant precipitation	N/A
6:2	Granular	10.28 ± 2.40	Some precipitation	N/A
FD protocol	**All samples prepared with fixed Man: Suc at 6/2 %w/v**			
Unannealed	Granular with large aggregates	10.28 ± 2.40	Some precipitation	N/A
Conservative	Fine powder	4.47 ± 1.13[a]	Completely soluble	3.28 ± 0.49
Extensive	Fine powder	4.09 ± 0.91[b]	Completely soluble	2.52 ± 0.81

[a, b] Residual moisture content was lower than that of unannealed FD samples, $p < .05$.

Table 4. pH and gelation time of medicated CS/DHO lyophilizates after reconstitution.

Formula	CS (%w/v)	DHO (%w/v)	pH	Gelation time
F1	1.8	1.5	7.32 ± 0.06	6.19 ± 2.74
F2	1.8	2.0	7.44 ± 0.13	5.14 ± 1.23
F3	1.8	2.5	7.58 ± 0.05	2.84 ± 0.66
F4	1.4	1.5	6.96 ± 0.08	15.55 ± 4.73
F5	1.4	2.0	7.15 ± 0.04	10.50 ± 1.26
F6	1.4	2.5	7.11 ± 0.16	9.26 ± 3.51

A.

B. (i)   (ii)   (iii)
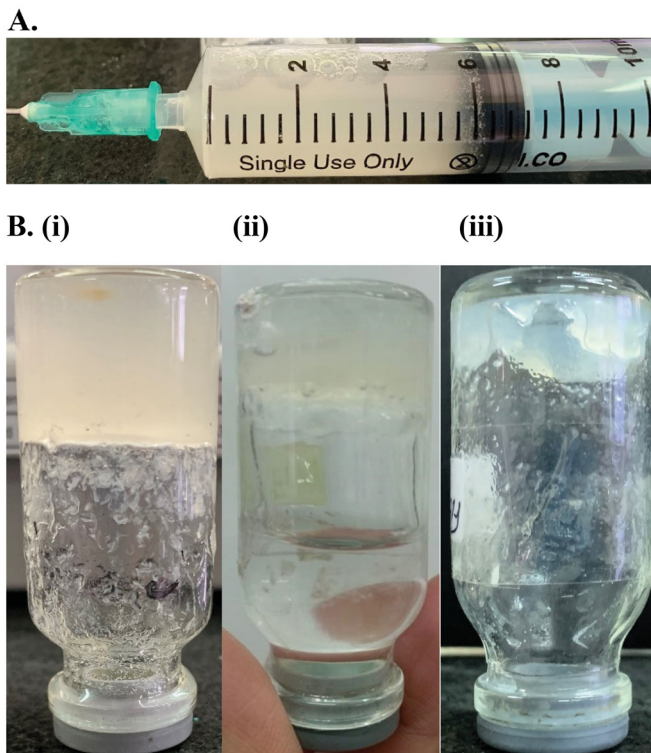
Figure 2. Representative procedure of the release experiment. (A) reconstitution of the lyophilizate and (B) The sample at the beginning (i), during (ii) and at the end (iii) of the release experiment.

inversely related to both CS and DHO concentration gelation times ranging from 2.84 ± 0.66 min for highest CS and DHO concentrations (F3) to 15.55 ± 4.73 min for lowest CS and DHO concentrations (F4). Samples prepared with CS 1.8%: F1, F2 and F3 showed shorter gelation times compared to samples prepared with CS 1.4%: F4, F5 and F6 respectively ($p < .05$). Likewise, the gelation time was noted to shorten with increasing DHO concentration where a significantly lower gelation time was noted for F3 compared to F1 and F2 ($p < .05$) as well as, F6 compared to F4 and F5 ($p > .05$). As

presented in Table 4, the pH of the studied formulations ranged from 6.96 ± 0.08 to 7.58 ± 0.05. The system demonstrated thermo-reversibility for all formulations when equilibrated to ambient temperature for 15 min.

4.4. In-vitro release study

Figure 2(A) displays representative sample reconstitution as well as at the beginning, during and at the end of the release experiment (Figure 2(B) i, ii, and iii respectively). As illustrated in Figure 4, TP release rate was markedly faster at pH 6.5 compared to pH 7.4 for both F1 and F2. A significant burst release of 42.5% and 30% occurred within 2 hrs for F1 and F2, respectively which plateaued at 75% after 12 hrs, and 60% after 24 hrs, respectively (Figure 3). Of note, the release profile for F2 was significantly slower than F1 at pH 6.5 for all sampling time points. Interestingly, F1 and F2 showed a very similar release profile at all time points at pH 7.4. As indicated in Figure 4, the release rate was much more prolonged with only ∼25% release within 2 hrs.

To study the effect of varying system component concentrations, the TP release behavior was studied at two CS concentrations and three DHO concentrations (Figure 4(A–C)). Formulae prepared with 1.5% w/v CS (F4 – F6) showed a relatively faster release when compared to formulations containing 2%w/v CS (F1 – F3) for each DHO concentration. The difference was statistically significant for pairwise comparison of F1 vs. F4 and F2 vs. F5 with 10% faster release rate noted for both F4 and F5. There was no statistically significant difference between the release of F3 compared to F6. On the other hand, at a fixed CS concentration of 1.5% w/v, and varying DHO concentrations, an insignificant difference ($p > .05$) in the release rate was detected for F4 – F6. Whereas, at a higher CS level (2% w/v), F1, F2 and F3 showed a decreasing release rate with increasing DHO concentration at a $p < .05$. The PDGF-BB release profile for the above-mentioned formulations showed a similar trend (Figure 4(D–F)). Interestingly, on comparison of TP release to PDGF-BB release for any given formulation, the later was released at a faster rate. This difference was significant for all time points throughout the experiment for formulations F1 – F6.

To further understand the above results, the release data were fitted to several kinetic models using KinetDS. As depicted in Table 5, TP and PDGF-BB release data fitted to a Higuchi model with an r^2 value of 0.9838 and 0.9860, respectively. This was reinforced with a Korsmeyer Peppas fit
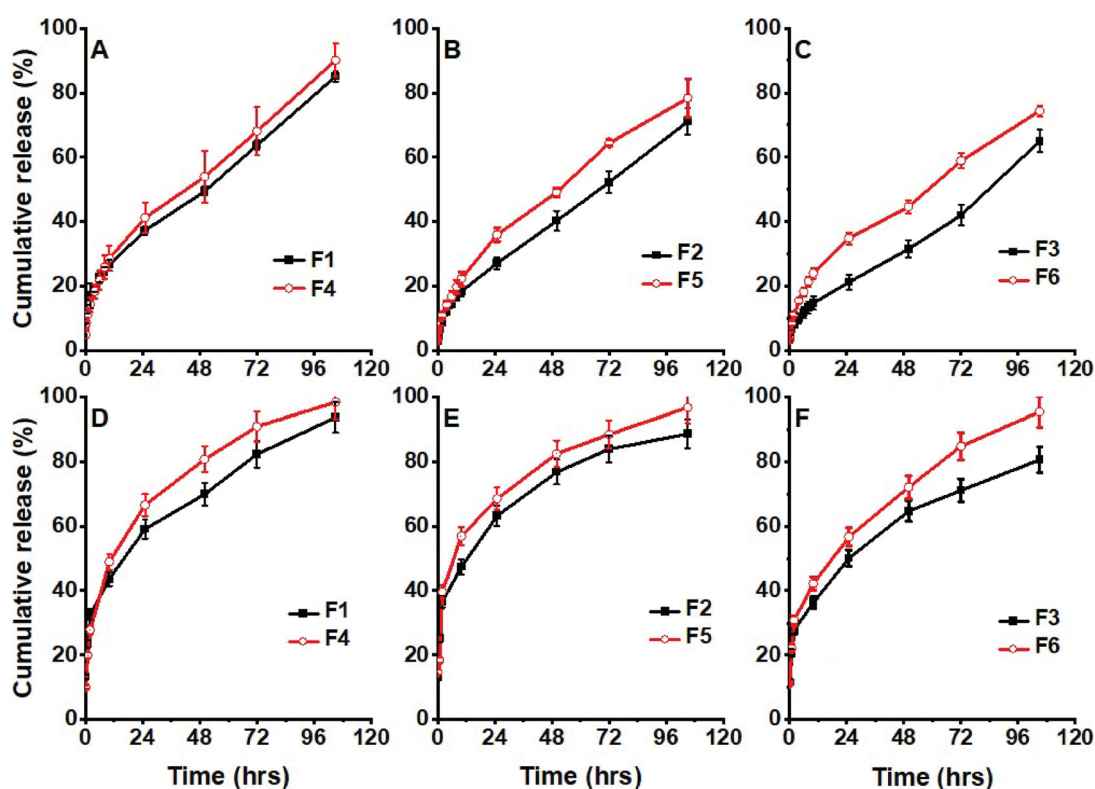
Figure 4. Release profile for Total protein. (A) F1 vs F4, (B) F2 vs. F5, (C) F3 vs. F6, and (D) PDGF-BB F1 vs F4, (E) F2 vs. F5, (F) F3 vs. F6 at a fixed DHO concentration of 1.5, 2 and 2.5%w/v, respectively.
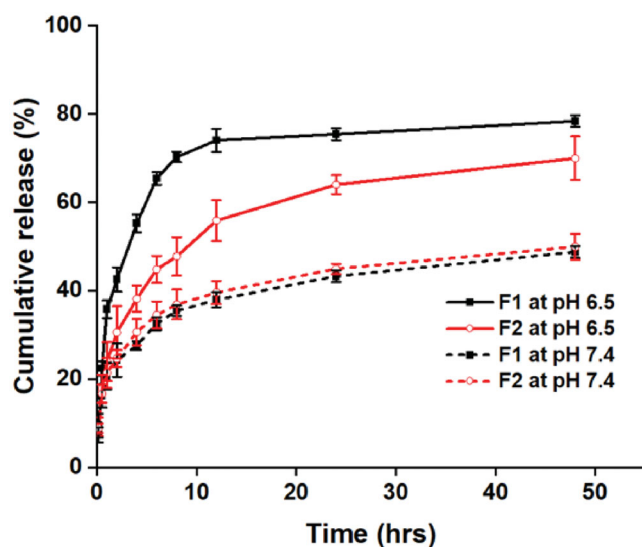
Figure 3. Total protein release profile of F1 and F2 at pH 6.5 and 7.4.

with n-values of 0.4982 and 0.3865, respectively. The computed r^2 for Weibull and Hixson Crowell kinetic models are as indicated in Table 5.

4.5. Cytotoxicity assay

Cytotoxicity testing on HSF indicated the formulation was highly safe. At a concentration of 100 μg/mL, cell viability was 78.5% ± 0.25% which reflects a half-maximal inhibitory concentration (IC50) greater than 100 μg/mL. Illustrated in Figure 5 are photomicrographs of HSF cultured cell line

Table 5. Kinetic modeling of total protein and PDGF-BB release data.

| Kinetic Model	Total Protein r^2	PDGF-BB r^2
Zero Order	0.9793	0.8697
First Order	0.96	0.9565
Higuchi	*0.9838*	*0.9860*
Korsmeyer Peppas	*0.9976 (n = 0.4982)*	*0.9694 (n = 0.3865)*
Weibull	0.9775	0.7835
Hickson Crowell	0.8253	0.7090

r^2 is the correlation coefficient and n is the release exponent.

using a blank formulation as control and F3 with 100 μg/mL HPL showing a healthy appearance of fibroblasts.

4.6. Stability of CS/DHO lyophilizate

All stability samples showed a similar physical appearance with no apparent aggregation. All formulations demonstrated good storage stability at 4 °C for 6 months. Analysis of reconstituted samples showed an insignificant change of PDGF-BB bioactivity at all sampling timepoints. Specifically, PDGF-BB bioactivity was between 90.01 ± 3.57% to 103.5 ± 3.41% of baseline PDGF-BB bioactivity at day 0 of the experiment.

5. Discussion

The lack of standardization of PRP products and a variation in quality based on intra- and inter-individual differences in blood composition is a standing issue (Chahla et al., 2017). Summoned to the bolus release of GFs and lack of stability, and in light of its considerable wound healing properties

A.   **B.**
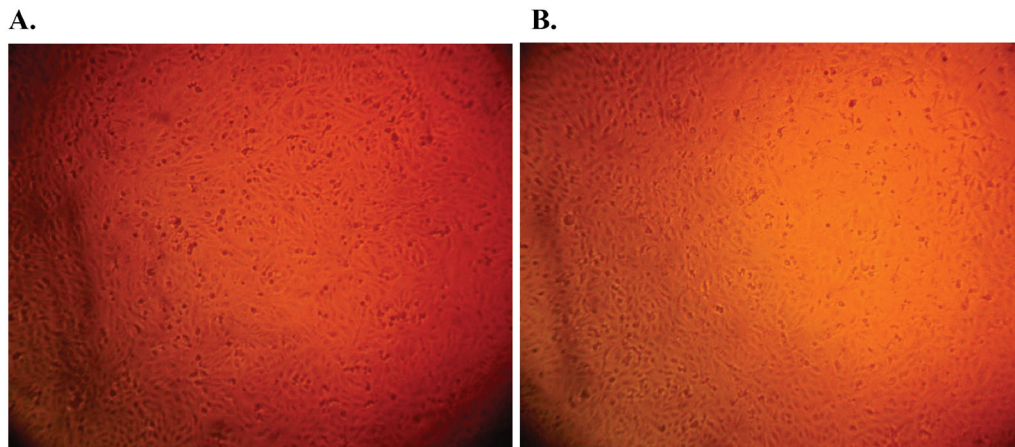
Figure 5. Cytotoxicity testing of F3. Photomicrograph showing the viability of HSF cells cultured in direct contact with a CS/DHO gel prepared with 1.8% CS and 2% DHO at a HPL concentration of: (A) 0 μg/mL and (B) 100 μg/mL.

there is a significant room for enhancement. Few attempts to produce a standardized controlled release PRP delivery systems have been made including loading PRP or its derivatives into hydrogels (Censi et al., 2020), smart wound dressings (Rossi et al., 2013), nanoparticulate or nanofiber systems (Cheng et al., 2018). A lyophilized platelet lysate based on apheresis PC was first produced by Kieb *et al* (Kieb et al., 2017). Based on GF testing in PRP derivatives prepared using four different techniques, the authors reported the highest GF concentrations in lyophilized PRP powder. In light of this, we were prompted to prepare lyophilized HPL using apheresis leukocyte-reduced PC and then formulate it into a novel lyophilized thermo-sensitive hydrogel system. ELISA testing of HPL confirmed α-particle degranulation and release of GF as indicated by the increase in PDGF-BB content compared to fresh PC samples. This signifies efficient lysis of platelets using three consecutive freeze-thaw cycles which is in consensus with previous studies (Strandberg et al., 2017). In addition, comparative analysis of HPL and lyophilized HPL revealed no detrimental effect of freeze-drying on the biochemical stability of PDGF-BB.

Despite the immense importance of CS as a highly biocompatible polymer that is frequently used in biomedical applications, CS/di-anionic thermo-responsive systems showed two main drawbacks: spontaneous gelation upon short-term storage at ambient or refrigerated conditions, and sparsity of long-term biological stability studies (Ruel-Gariépy et al., 2000). Wu *et al* fabricated a lyophilized CS/β-GP thermogel system with the intention to overcome existing limitations (Wu et al., 2016). One challenge that the authors faced was the precipitation of the system on reconstitution due to FD-induced premature cross-linking of CS to β-GP. To the best of our knowledge, this was the only attempt to formulate a lyophilized form of a CS/di-anionic thermogel.

FD is a technique that is often employed to maximize the shelf-life of biologics (Cao et al., 2013). The use of adequate bulking and stabilizing agents' levels as well as refinement of FD conditions is crucial for the production of a pharmaceutically acceptable product (Hansen et al., 2015). Therefore, optimization of the FD conditions and the use of appropriate excipients is critical (Awotwe-Otoo et al., 2012). For

cryoprotectant optimization experiments, an unannealed FD procedure was used where, samples were frozen at $-20\,°C$ and freeze-dried for 12 hrs. Results presented for Man: Suc contents of 4:1 and 4:2%w/v, indicate that the residual moisture content exceeded the pre-set limit of 5%. Moreover, for all cryoprotectant levels tested, samples showed prominent cake collapse, sticky appearance and failed to re-dissolve completely.

Annealing is a process by means of which induction of crystallization of the bulking agent is achieved via manipulating Tp. This triggers ice nucleation in the product through a process referred to as "Ostwald ripening" (Kumar et al., 2019). Adopting this concept, samples prepared using conservative annealing procedure were subjected to low-temperature annealing during the freezing stage at $-20\,°C$ above the glass transition temperature, $Tg_□$ of frozen Man solution reported to be at around $-35\,°C$. This induces Man crystallization above its $Tg_□$ yet sufficiently below its collapse temperature (Tc) at $-1.5\,°C$ (Remmele et al., 2012). During primary drying, the product temperature was controlled at the sublimation interface below $Tg_□$. This was achieved by quickly placing samples frozen at $-45\,°C$ in the freeze-dryer and immediately applying vacuum. This precluded the Tp from rising beyond $Tg_□$, hence avoiding cake collapse. Moreover, samples prepared using extensive annealing procedure were subjected to low- and high- temperature annealing during freezing and secondary drying stages, respectively. During secondary drying, lyophilized cakes were subjected to vacuum drying at ambient temperature. The same rationale applies, where dry amorphous Man is reported to have a Tg of $12\,°C$, while that of amorphous Suc is reported at $52–70\,°C$ (Horn et al., 2018). High-temperature annealing during secondary drying has been reported to induce further crystallization of Man that may have retained its amorphous form during freezing (Bjelošević et al., 2020). It is critical that high-temperature annealing is executed at a temperature below the Tg of Suc to prevent product micro-collapse.

In light of the above, we speculate that the lack of an annealing step and Tp of $-20\,°C$, well above the $Tg_□$ of Man, at the beginning of primary drying may have

compromised product CQAs in samples subjected to unannealed FD. The above results reinforce previous findings of Horn et al who concluded that final product characteristics were most sensitive to the FD procedures, particularly annealing steps rather than the Man: Suc ratio used for the preparation of the samples (Horn et al., 2018). From the above, we were able to achieve an elegant, lyophilized product with acceptable residual moisture and a reasonable reconstitution time.

In addition to the product CQA optimization mentioned above, it was indispensable to undertake thermal behavior, vibrational spectroscopy, and morphological analyses. The DSC thermogram obtained for the lyophilizate system confirmed the absence of the crystallization exotherm of Man. This indicates that Man created a thermally stable crystalline scaffold in the cake which was our goal for the FD optimization (Jena et al., 2019). In addition, a low energy step-down transition signified a Tg at around 45 °C. Since previous reports suggested optimal storage temperatures for freeze-dried formulations to be at least 10–20 °C lower than the Tg, our results forecast adequate product stability at convenient storage conditions (Grasmeijer et al., 2013).

Morphological analysis of the system using XRPD enabled the resolution of Man polymorphs existent in the lyophilizate system. The obtained X-ray diffractograms confirmed the predominance of β-Man in the lyophilizate system over metastable polymorphs namely, α, β, δ and Man hemihydrate. We predict that this may have been facilitated by the relatively low protein concentration in the formula at 1% w/v, with a Man concentration of 6% w/v. This is in compliance with similar studies implementing annealed FD protocols to maximize Man crystallization (Rodrigues et al., 2021).

Preservation of the native protein structure is a result of two main processes that occur during FD namely, 1) water substitution by sucrose as a stabilizer, and 2) molecular immobilization due to freezing, also known as vitrification. However, freeze-concentration and dehydration stresses can impose significant perturbations on the conformational stability of protein molecules (Mensink et al., 2017). FT-IR spectroscopy has long been used to study stress-induced alterations in protein conformation, where, band positions are used to determine landmark functional groups present in a protein, specifically amide I and II (Murayama and Tomida, 2004). The FT-IR spectrum of HPL-loaded F3 lyophilizate manifested similar band positions when collated against FT-IR spectra of HPL alone and CS alone. Particularly, amide I and II absorbance bands were almost superimposed to the native bands projected by pure HPL. This indicates that the carbonyl (C=O) stretching vibration, coupled with C–N stretching and N–H bending were not affected by the formulation and processing of the product. The above findings confirm adequate vitrification and stabilization by sucrose hydrogen-bonding in place of water as reported by similar studies (Remmele et al., 2012). However, a slight shift of the amide I peak from 1544 to 1568 cm^{-1} may indicate a possible interaction between the amino groups of CS backbone and HPL GFs that is probably hydrophobic in nature (Stodolak-Zych et al., 2020). Concluding the above system design and

optimization, optimized lyophilizates of F1 to F6 were prepared with Man: Suc of 6:2%w/v and an extensive FD procedure for subsequent system characterization.

Depending on the CS and DHO concentrations, the gelation time was found to be adjustable for a certain utility. In line with previous reports, results presented for gelation time indicate a reverse relation with both CS and DHO concentration (Li et al., 2011; Casettari et al., 2013). This is most likely attributed to less thermal energy required to induce sol-to-gel transition at higher CS concentrations. Similarly, at a higher DHO concentration, a shorter gelation time was noted most probably due to a larger increase in pH near the precipitation point of CS (Ta et al., 2009). It is important to note, that gel dispersions prepared with higher CS and DHO had a higher baseline viscosity. This feature allows adjustability of the system by manipulating CS and DHO concentrations, to target a desired thermogelling time, or thermogelling temperature (Ta et al., 2009). This may have applicability in different wound types such as musculoskeletal injuries at core body temperature as opposed to superficial injuries such as skin ulcerations or burns. Apparently, all the prepared formulations exhibited thermo-reversibility of the CS/DHO hydrogels when equilibrated to ambient temperature. This may be ascribed to the competition between the weak hydrophobic forces which are known to be temperature dependent (Lavertu et al., 2008).

In-vitro release and the impact of reactant concentrations and pH on the release behavior of TP and PDGF-BB were investigated. As shown in Figure 4, all formulations demonstrated a biphasic release behavior for both TP and PDGF-BB. The initial burst release within 2 hours may be attributed to the immediate dissolution and release of HPL proteins accumulated on the surface of the thermogel which could diffuse rapidly once in contact with the release medium. Beyond this burst, the release pattern was sustained over five days.

Moreover, the release behavior was found to be significantly affected by pH. In an acidic pH closer to its pKa, CS is more protonated, which causes it to dissolve and the system to erode faster (Ta et al., 2009). Consequently, at pH 6.5, F1 and F2 showed a significant burst release of 42.5% and 30% respectively within 2 hrs whereas, at pH 7.4, the TP content was gradually eluted with only 24% and 20% release in the first 2 hrs, respectively. Further, the marked difference in release rate between F1 and F2 shown at pH 6.5 was alleviated as the pH increased to 7.4 (Wu et al., 2016).

It could be concluded therefore that protein release at pH < pKa of CS is majorly dependent on gel erosion, whereas a much slower release rate at higher pH signifies diffusion-dependent release (Bhattarai et al., 2005). These results are in good correlation with results reported by Wu et al (Wu et al., 2016).

Furthermore, CS concentration had a more pronounced effect on the release pattern in contrast to DHO concentration. As shown in Figure 4(A–C), at all DHO concentrations, F4, F5 and F6 (CS 1.4%) manifested a faster TP release compared to CS 1.8% in F1, F2 and F3, respectively. This result indicates that CS concentration governs the release rate of the system. In contrast, at a fixed CS concentration, varying

DHO concentration did not have a marked impact on the release rate, where F4, F5 and F6 showed very similar release profiles ($\rho > .05$) and F1, F2 and F3 only showed a 10% faster TP release rate with decreasing DHO concentration. Similar release trends were observed for PDGF-BB as illustrated in Figure 4(D–F). The above findings are in line with the earlier reports (Ta et al., 2009).

Protein diffusivity is dependent on a variety of factors such as protein size (MW and hydrodynamic radius), isoelectric point (pI) as well as hydrogel mesh size. As indicated in Table 5, TP and PDGF-BB release data fitted best to a Higuchi model indicating diffusion-based release with $r^2 = 0.9838$ and 0.9860, respectively. Korsmeyer-Peppas fit computed an n-value close to 0.5 for TP release, indicating that the release followed a coupled diffusion-erosion mode. Interestingly, Korsmeyer-Peppas fit of PDGF-BB release data resulted in an n-value of 0.39. This may stipulate that Fickian diffusion dominated the release behavior for this particular GF through the hydrogel matrix. PDGF-BB has a M.W. of 27 kDa with a relatively small hydrodynamic radius while other plasma proteins are much larger e.g., fibrinogen, hepatocyte growth factor (HGF), and albumin have M.W. of 340, 92 and 66 KDa, respectively (Sellberg et al., 2016). As a result, PDGF-BB could easily diffuse out of the hydrogel matrix in a Fickian manner. Conversely, the TP content has a much higher average M.W. which was impeded by marked steric hindrance by the thermogel mesh during release. Similar results were reported using different model proteins such as lysozyme and albumin (Drinnan et al., 2010; Jain et al., 2019).

One of the simplest biological characterization techniques of potential tissue regeneration materials is cytotoxicity evaluation (Lee et al., 2000). The cytotoxicity of the system was tested on the HSF cell line since the system was developed primarily for wound healing applications. As expected, the lyophilizate system presented encouraging cell viability results with similar absorbance of investigated hydrogel and negative control indicating no harmful effect. This is attributed to its highly biocompatible composition and mild formulation procedures undertaken.

Based on our stability testing, the CS/DHO lyophilizate system achieved its goal of preservation of protein bioactivity for a shelf-life of 6 months when stored in refrigerated conditions. Samples analyzed using ELISA at pre-set time-points showed relative stability in PDGF-BB bioactivity with no significant difference detected at any sampling time point. This therefore indicates the structural stability of PDGF-BB as a representative GF. These results may be extrapolated to the overall GF composition of HPL. This may be further studied using multiplex ELISA kits to detect several GFs. Moreover, none of the samples showed any physical changes such as hydration or clumping despite not using a desiccator.

6. Conclusion

The long-term dry stabilization of PRP and its derivatives can dramatically change the practice of their use for wound-healing applications in several clinical settings. The developed system overcomes the drawbacks of currently used PRP treatment techniques and provides a novel HPL-loaded scaffold for wound repair. We succeeded to engineer a highly biocompatible controlled release system of GF-rich allogeneic HPL. The system shows promise for use in wound healing, especially chronic non-healing wounds or difficult-to-access injury sites. The system exhibits a practical stability profile and is easy to use. The insights gained may open a new paradigm on the use of this potential delivery system which will be further investigated *in vivo* and clinically, as future scope.

Data availability statement

The data that support the findings of this study are available from the corresponding author, Toaa A. Abdelrahman, upon reasonable request.

References

Cao W, Krishnan S, pee. Ricci MS, et al. (2013). Rational design of lyophilized high concentration protein formulations-mitigating the challenge of slow reconstitution with multidisciplinary strategies. Eur J Pharm Biopharm 85:287–93.

Amable PR, Bizon R, Carias V, et al. (2013). Platelet-rich plasma preparation for regenerative medicine: optimization and quantification of cytokines and growth factors. Stem Cell Res Ther 4:67.

Anitua E, Alkhraisat MH, Orive G. (2012). Perspectives and challenges in regenerative medicine using plasma rich in growth factors. J Control Release 157:29–38.

Anitua E, MD DDS, de la Fuente M, et al. (2015). Preservation of biological activity of plasma and platelet-derived eye drops after their different time and temperature conditions of storage. Cornea 34: 1144–8. , http://ovidsp.ovid.com/ovidweb.cgi?T=JS&PAGE=reference& D=ovftq&NEWS=N&AN=00003226-201509000-00026.

Anitua E, Muruzabal F, Pino A, et al. (2013). Biological stability of plasma rich in growth factors eye drops after storage of 3 months. Cornea 32:1380–6.

Assegehegn G, Brito-de la Fuente E, Franco JM, Gallegos C. (2020). Use of a temperature ramp approach (TRA) to design an optimum and robust freeze-drying process for pharmaceutical formulations. Int J Pharm 578:119116.

Awotwe-Otoo D, Agarabi C, Wu GK, et al. (2012). Quality by design: impact of formulation variables and their interactions on quality attributes of a lyophilized monoclonal antibody. Int J Pharm 438: 167–75.,.

Belk JW, Kraeutler MJ, Houck DA, et al. (2021). Platelet-rich plasma versus hyaluronic acid for knee osteoarthritis: a systematic review and meta-analysis of randomized controlled trials. Am J Sports Med 49:249–60.

Bernal-Chávez SA, Alcalá-Alcalá S, Cerecedo D, Ganem-Rondero A. (2020). Platelet lysate-loaded PLGA nanoparticles in a thermo-responsive hydrogel intended for the treatment of wounds. Eur J Pharm Sci 146: 105231.

Bhattarai N, Ramay HR, Gunn J, et al. (2005). PEG-grafted chitosan as an injectable thermosensitive hydrogel for sustained protein release. J Control Release 103:609–24.

Bjelošević M, Zvonar Pobirk A, Planinšek O, Ahlin Grabnar P. (2020). Excipients in freeze-dried biopharmaceuticals: Contributions toward formulation stability and lyophilisation cycle optimisation. Int J Pharm 576:119029.

Bullock AJ, Garcia M, Shepherd J, et al. (2020). Bacteria induced pH changes in tissue-engineered human skin detected non-invasively using Raman confocal spectroscopy. Appl Spectrosc Rev 55:158–71.

Carter MJ, Fylling CP. (2011). Use of platelet rich plasma gel on wound healing: a systematic review and meta-analysis. Eplasty 11:e38.

Casettari L, Cespi M, Palmieri GF, Bonacucina G. (2013). Characterization of the interaction between chitosan and inorganic sodium phosphates by means of rheological and optical microscopy studies. Carbohydr Polym 91:597–602.

Censi R, Casadidio C, Deng S, et al. (2020). Interpenetrating hydrogel networks enhance mechanical stability, rheological properties, release behavior and adhesiveness of platelet-rich plasma. IJMS 21:1399.

Chahla J, Cinque ME, Piuzzi NS, et al. (2017). A call for standardization in platelet-rich plasma preparation protocols and composition reporting: a systematic review of the clinical orthopaedic literature. J Bone Joint Surg Am 99:1769–79.

Cheng G, Ma X, Li J, et al. (2018). Incorporating platelet-rich plasma into coaxial electrospun nanofibers for bone tissue engineering. Int J Pharm 547:656–66.

Chenite A, Chaput C, Wang D, et al. (2000). Novel injectable neutral solutions of chitosan form biodegradable gels in situ. Biomaterials 21:2155–61.

Drinnan CT, Zhang G, Alexander MA, et al. (2010). Multimodal release of transforming growth factor-β1 and the BB isoform of platelet derived growth factor from PEGylated fibrin gels. J Control Release 147:180–6.

Fekete N, Gadelorge MÉL, Rst DFÜ, et al. (2012). Platelet lysate from whole blood-derived pooled platelet concentrates and apheresis-derived platelet concentrates for the isolation and expansion of human bone marrow mesenchymal stromal cells: production process, content and identification of active components. Cytotherapy 14:540–54.

Fernandez-Moure JS, Van Eps JL, Cabrera FJ, et al. (2017). Platelet-rich plasma: a biomimetic approach to enhancement of surgical wound healing. J Surg Res 207:33–44.

Grasmeijer N, Stankovic M, De Waard H, et al. (2013). Unraveling protein stabilization mechanisms: Vitrification and water replacement in a glass transition temperature controlled system. Biochim Biophys Acta - Proteins Proteomics 1834:763–9.

Haeuser C, Goldbach P, Huwyler J, et al. (2020). Impact of dextran on thermal properties, product quality attributes, and monoclonal antibody stability in freeze-dried formulations. Eur J Pharm Biopharm 147:45–56.

Hansen LJJ, Daoussi R, Vervaet C, et al. (2015). Freeze-drying of live virus vaccines: a review. Vaccine 33:5507–19.

He M, Guo X, Li T, et al. (2020). Comparison of allogeneic platelet-rich plasma with autologous platelet-rich plasma for the treatment of diabetic lower extremity ulcers. Cell Transplant 29:963689720931428–9.

Higuchi T. (1963). Mechanism of sustained-action medication. theoretical analysis of rate of release of solid drugs dispersed in solid matrices. J Pharm Sci 52:1145–9.

Hixson AW, Crowell JH. (1931). Dependence of reaction velocity upon surface and agitation: III—experimental procedure in study of agitation. Ind Eng Chem 23:1160–8.

Horn J, Schanda J, Friess W. (2018). Impact of fast and conservative freeze-drying on product quality of protein-mannitol-sucrose-glycerol lyophilizates. Eur J Pharm Biopharm 127:342–54.

Jain E, Chinzei N, Blanco A, et al. (2019). Platelet-rich plasma released from polyethylene glycol hydrogels exerts beneficial effects on human chondrocytes. J Orthop Res 37:2401–10.

Jain E, Sheth S, Dunn A, et al. (2017). Sustained release of multicomponent platelet-rich plasma proteins from hydrolytically degradable PEG hydrogels. J Biomed Mater Res A 105:3304–14.

Jena S, Krishna Kumar NS, Aksan A, Suryanarayanan R. (2019). Stability of lyophilized albumin formulations: Role of excipient crystallinity and molecular mobility. Int J Pharm 569:118568.

Kieb M, Sander F, Prinz C, et al. (2017). Platelet-rich plasma powder: a new preparation method for the standardization of growth factor concentrations. Am J Sports Med 45:954–60.

Korsmeyer RW, Gurny R, Doelker E, et al. (1983). Mechanisms of solute release from porous hydrophilic polymers. Int J Pharm 15:25–35.(83)90064-9.

Kumar L, Chandrababu KB, Balakrishnan SM, et al. (2019). Optimizing the Formulation and Lyophilization Process for a Fragment Antigen Binding (Fab) Protein Using Solid-State Hydrogen-Deuterium Exchange Mass Spectrometry (ssHDX-MS). Mol Pharmaceutics 16:4485–95.

Langenbucher F. (1972). Letters to the Editor: Linearization of dissolution rate curves by the Weibull distribution. J Pharm Pharmacol 24:979–81.

Lavertu M, Filion D, Buschmann MD. (2008). Heat-induced transfer of protons from chitosan to glycerol phosphate produces chitosan precipitation and gelation. Biomacromolecules 9:640–50.

Lee JK, Kim DB, Il Kim J, Kim PY. (2000). In vitro cytotoxicity tests on cultured human skin fibroblasts to predict skin irritation potential of surfactants. Toxicol. Vitr 14:345–9.(00)00028-X.

Lewis LM, Johnson RE, Oldroyd ME, et al. (2010). Characterizing the freeze-drying behavior of model protein formulations. AAPS Pharm Sci Tech 11:1580–90.

Li XY, Kong XY, Zhang J, et al. (2011). A novel composite hydrogel based on chitosan and inorganic phosphate for local drug delivery of camptothecin nanocolloids. J Pharm Sci 100:232–41.

Liu L, Gao Q, Lu X, Zhou H. (2016). In situ forming hydrogels based on chitosan for. Asian J Pharm Sci 11:673–83.

Marx RED. (2001). Platelet-Rich Plasma (PRP): What is PRP and what is not PRP? Implant Dent 10:225–8.

Mendyk A, Jachowicz R, Fijorek K, et al. (2012). KinetDS: an open source software for dissolution test data analysis. Dissolution Technol 19:6–11.

Mensink MA, Frijlink HW, van der Voort Maarschalk K, Hinrichs WLJ. (2017). How sugars protect proteins in the solid state and during drying (review): Mechanisms of stabilization in relation to stress conditions. Eur J Pharm Biopharm 114:288–95.

Murayama K, Tomida M. (2004). Heat-induced secondary structure and conformation change of bovine serum albumin investigated by Fourier transform infrared spectroscopy. Biochemistry 43:11526–32.

Nair LS, Starnes T, Ko JWK, Laurencin CT. (2007). Development of injectable thermogelling chitosan-inorganic phosphate solutions for biomedical applications. Biomacromolecules 8:3779–85.

Oneto P, Etulain J, Oneto P, Etulain J. (2021). PRP in wound healing applications PRP in wound healing applications. Platelets 32:189–11.

Rathore N, Rajan RS. (2008). Current perspectives on stability of protein drug products during formulation, fill and finish operations. Biotechnol Prog 24:504–14.

Remmele RL, Krishnan S, Callahan WJ. (2012). Development of Stable Lyophilized Protein Drug Products. Curr Pharm Biotechnol 13:471–96.

Rodrigues MA, Rego P, Geraldes V, et al. (2021). Mannitol crystallization at sub-zero temperatures: time/temperature-resolved synchrotron X-ray diffraction study and the phase diagram. J Phys Chem Lett 12:1453–60.

Rossi S, Faccendini A, Bonferoni MC, et al. (2013). "Sponge-like" dressings based on biopolymers for the delivery of platelet lysate to skin chronic wounds. Int J Pharm 440:207–15.

Ruel-Gariépy E, Chenite A, Chaput C, et al. (2000). Characterization of thermosensitive chitosan gels for the sustained delivery of drugs. Int J Pharm 203:89–98.(00)00428-2.

Santana H, Sotolongo J, González Y, et al. (2014). Stabilization of a recombinant human epidermal growth factor parenteral formulation through freeze-drying. Biologicals 42:322–33.

Schallmoser K, Strunk D. (2009). Preparation of pooled human platelet lysate (pHPL) as an efficient supplement for animal serum-free human stem cell cultures. J Vis Exp 32:1523.

Sellberg F, Berglund E, Ronaghi M, et al. (2016). Composition of growth factors and cytokines in lysates obtained from fresh versus stored pathogen-inactivated platelet units. Transfus Apher Sci 55:333–7.

Stodolak-Zych E, Jeleń P, Dzierzkowska E, et al. (2020). Modification of chitosan fibers with short peptides as a model of synthetic extracellular matrix. J Mol Struct 1211:128061.

Strandberg G, Sellberg F, Sommar P, et al. (2017). Standardizing the freeze-thaw preparation of growth factors from platelet lysate. EDITORIAL 57:1058–7.,.

Sumner SM, Naskou MC, Thoresen M, et al. (2017). Platelet lysate obtained via plateletpheresis performed in standing and awake equine donors. J AAB Tranfusion 57:1755–62.

Sundman EA, Cole BJ, Fortier LA, et al. (2011). Growth factor and catabolic cytokine concentrations are influenced by the cellular composition of platelet-rich plasma. Am J Sports Med 39:2135–40.

Ta HT, Han H, Larson I, et al. (2009). Chitosan-dibasic orthophosphate hydrogel: A potential drug delivery system. Int J Pharm 371:134–41.

U.S. Department of Health and Human Services Food and Drug Administration (2009). ICH Q8(R2) Pharmaceutical Development. Work Qual by Des. Pharm 8:28.,

Wu G, Yuan Y, He J, et al. (2016). Stable thermosensitive in situ gel-forming systems based on the lyophilizate of chitosan/α,β-glycerophosphate salts. Int J Pharm 511:560–9.